



*Anal. Bioanal. Chem. Res., Vol. 11, No. 2, 123-137, April 2024.*

## Optimization of Removal of Ibuprofen Antibiotic from Water in the Presence of ZnO/Fe<sub>2</sub>O<sub>3</sub> and ZnO/activated Carbon Nanoparticles Using Response Surface Methodology

Ehsan Amirmotalebi, Naser Samadi\* and Sohrab Ershad

*Department of Analytical Chemistry, Faculty of Chemistry, Urmia University, Urmia, Iran*

*(Received 26 September 2023, Accepted 7 December 2023)*

In this study, ZnO/Fe<sub>2</sub>O<sub>3</sub> and ZnO/activated carbon nanoparticles were used as efficient adsorbents for the removal of the antibiotic ibuprofen from aqueous solutions. The nanoadsorbents were characterized by X-ray diffraction (XRD), scanning electron microscopy (SEM), transmission electron microscopy (TEM), Fourier-transform infrared spectroscopy (FTIR), and Brunauer–Emmett–Teller (BET) analyses. The results show that the ZnO/Fe<sub>2</sub>O<sub>3</sub> and ZnO/activated carbon nanocomposites were successfully synthesized. Optimization of ibuprofen removal was investigated using response surface methodology (RSM) based on central composite design (CCD). The process parameters such as the pH (4-6), contact time (10-20 min), nanoparticle dosage (0.02-0.04 wt.%), and type of nanoadsorbent (ZnO/Fe<sub>2</sub>O<sub>3</sub> and ZnO/activated carbon) were investigated in batch experiments. Within the range of the selected experimental conditions, the optimum values for pH, contact time, nanoparticle dosage, and nanoadsorbent type were found to be 5.48, 17.22 min, 0.03 wt.% and ZnO/Fe<sub>2</sub>O<sub>3</sub>, respectively. Under the optimal conditions, the expected ibuprofen removal was 83.74% and the empirical value was 85.42%. The high values of R<sup>2</sup> 0.9596 and R<sup>2</sup> adj 0.9378 indicate that the fitted model has satisfactory agreement with the expected and empirical ibuprofen removal. The adsorption kinetics and isotherms are well fitted with the pseudo-second-order and Langmuir models, respectively, implying that the single-layer adsorption of ibuprofen on the surface of the adsorbent is controlled by electrostatic interactions, stacking of  $\pi$ - $\pi$  and hydrogen bonding.

**Keywords:** ZnO/Fe<sub>2</sub>O<sub>3</sub>, ZnO/activated carbon, Adsorption isotherms, Ibuprofen, Optimization, Response surface methodology

### INTRODUCTION

Due to the increasing population growth and the rapid development of industry and technology, the increasing demand for potable water and the shortage of potable water resources have become a global challenge [1]. This increase in demand has led to various solutions to address this problem. In addition to the problems related to water scarcity, the presence of pollutants in aqueous solutions is also increasing with the expansion of industry [2]. This is due to uncontrolled discharge of industrial pollutants, disinfection of drinking water and treatment of wastewater with chlorine, hospital wastewater, leaching of fields contaminated with

chemical fertilizers by rainwater, or leakage of tanks containing materials [3,4]. One of the types of wastewater that are very dangerous in many cases is hospital wastewater, which contains harmful medical wastes that are not only dangerous to human health, but also, if reintroduced into the cycle of nature, have irreparable consequences for the environment, animals and plants [5]. Nowadays, antibiotics represent a high percentage of substances in hospital pollution [6]. The annual consumption of antibiotics in the world is estimated at 100,000 to 200,000 tons. Antibiotics are rarely completely degraded in the body after use, and 30 to 90% of them remain active after excretion [7]. It can be concluded that an average of 50,000 tons of active antibiotics are released into the environment each year. These compounds have been found in surface water, groundwater,

\*Corresponding author. E-mail: samadi76@yahoo.com

sewage, and even drinking water [8]. Medicinal compounds enter aqueous solutions through various sources such as the pharmaceutical industry, contaminants from hospitals, and human and animal excretions. The presence of antibiotics in the environment, including water and soil, even at low concentrations, leads to the development of antibiotic-resistant pathogens that potentially threaten ecosystem function and human health [9]. According to statistics in different parts of the world, the share of ibuprofen antibiotic (its chemical structure is illustrated in Fig. 1) is higher than other antibiotics. This antibiotic is widely used in the treatment of infectious diseases in hospitals. Therefore, it seems necessary to eliminate this pollutant from the aquatic environment by a logical method.

Adsorption is a physicochemical process in which liquid or gaseous molecules attach to a solid [10]. This process is based on the accumulation of substances at the interface between the two phases. In other words, the adsorption of molecules by the inner or outer surfaces of a solid can be considered surface adsorption [11]. Accordingly, one of these factors is the property of the adsorbent. Adsorption is a surface phenomenon and based on this principle, it can be stated that the amount of adsorption is proportional to the specific surface area of the adsorbent [12]. The specific surface area can be defined as the part of the total surface area that can be used for the adsorption process. The most important property of the adsorbent material is its specific surface. Adsorbents usually have many pores on the surface [13]. Therefore, the smaller the adsorbent particles are, the faster they come into contact with the liquid phase and the faster the process runs. In general, the more specific surface area the adsorbent has, the greater the adsorption capacity [14]. Nowadays, much attention is paid to the application of nanomaterials because they provide surface sites [15]. Hence, in the present study, ZnO/Fe<sub>2</sub>O<sub>3</sub> and ZnO/activated carbon nanoparticles were utilized as efficient nanoadsorbents. Therefore, the use of this nanoadsorbent together with the experimental design may be attractive in the absorption of drug impurities [16]. Experimental design is one way to improve the experimental conditions. The goal of experimental design is to gain maximum knowledge with a minimum number of experiments [17]. Experimental design involves explaining the effect of various factors as independent and adjustable input variables on the dependent

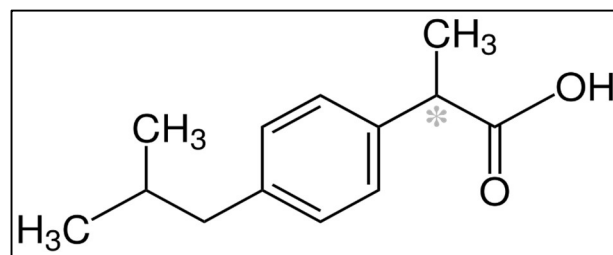


**Fig. 1.** Chemical structure of ibuprofen.

variable or output. Hence, the response surface methodology is a set of statistical techniques based on mathematics that is significantly applied in the design of experiments and optimization of chemical processes [18].

Removal of antibiotics from the aqueous solutions and synthesis of nanoparticles as a sorbent, due to their importance, is one of the most important areas of research. To our knowledge, the synthesis of ZnO/Fe<sub>2</sub>O<sub>3</sub> and ZnO/activated carbon nanoadsorbent for the removal of the ibuprofen antibiotic has not been carried out in an aqueous solution. Thus, the lack of study in this field is an incentive to conduct the present research. Besides, the effect of parameters affecting the separation of drug sewage such as pH, contact time, the dosage of nanoadsorbent, and nanoadsorbent type was investigated. Experimental design, statistical modeling, parameter interaction, and surface adsorption process optimization were performed using RSM and CCD. Therefore, the main aims of this research are: 1) synthesis of ZnO/Fe<sub>2</sub>O<sub>3</sub> and ZnO/activated carbon nanoadsorbents through the sol-gel approach. 2) Determining and identifying the structure of nanoparticles synthesized using XRD, SEM, and TEM techniques. 3) Investigating the effect of various parameters such as pH, contact time, the dosage of nanoadsorbent, and nanoadsorbent type on the value of removal of ibuprofen drug from the aqueous solutions. 4) statistical modeling of various operational parameters on the adsorption rate of drugs on solid nanopores, and 5) Investigating adsorption isotherms using Freundlich and Langmuir methods.

## EXPERIMENTAL

### Materials

The materials used in this research include iron nitrate,

zinc acetate, sodium hydroxide, activated carbon, ethanol, and nitric acid. It should be noted that all these materials were provided by Merck. Distilled water was also purchased as a solvent from Arman Sana Company. Moreover, ibuprofen (from the pharmacy located in Tehran, Iran) was also used as laboratory material for the synthesis of nanoadsorbent and the preparation of aqueous pollutants. Figure 1 depicts the chemical structure of ibuprofen.

### Synthesis of ZnO/Fe<sub>2</sub>O<sub>3</sub> Nano Adsorbent

ZnO/Fe<sub>2</sub>O<sub>3</sub> nanoadsorbent used in this research was synthesized according to the sol-gel route. "In the first step, 0.76 g of zinc acetate and 0.56 g of iron nitrate were dissolved in 20 ml of water and 10 ml of methanol, respectively". Afterward, stirring for 120 min on a magnetic stirrer, the two solutions were completely mixed together and then the pH of the solution was measured to determine the intensity of the play. Next, 1 molar sodium hydroxide solution is added dropwise to the solution until the mixture transfers pH = 10. Subsequently, the resulting mixture is poured into a Teflon autoclave, and then heated in an oven at 130 °C for 300 min. Afterward, after 120 min of cooling at the ambient temperature, the pH of the solution is measured again. The reddish-brown product is centrifuged for 20 min at 5000 rpm. Finally, the precipitate was dried at 150 °C for 180 min to obtain a nanoadsorbent [19].

### Synthesis of ZnO/activated Carbon Nano Adsorbent

The co-precipitation method was used to synthesize zinc oxide/activated carbon nanoparticles. In this method, aqueous salt solutions of Zn<sup>+2</sup> and in a molar ratio of 1:2 were mixed by increasing drop by drop of 1 molar sodium hydroxide. Then, 300 ml of deionized water was added and placed on a magnetic stirrer at 500 rpm for 30 min. Subsequently, a solution containing Zn<sup>+2</sup> ion was added to the solution being mixed. Afterward, at a certain time of stirring, sodium hydroxide solution was gradually added. Then, after 30 min, 1 g of activated carbon is combined with the solution and stirred for 60 min. Next, the resulting precipitate is washed with deionized water to remove impurities on the surface. This step is repeated 3 times until the pH of the washed solution reaches neutral. After the leaching operation, paste nanoparticles are obtained. Finally, the product is then dried in an oven at 80 °C for 8 h to obtain

a nanoabsorbent [19].

### Characterization of Nanoadsorbents

Synthesized nanoadsorbents have been identified by different procedures to analyze their morphology besides their structural characteristics. X-ray diffraction was performed on the DW-XRD-Y3000 Model XRD instrument over a 2θ domain of 10-80°. Scanning electron microscopy in order to detect morphology (SEM) was recognized with a layer of quorum model by EVO 18 Research, Carl Zeiss, UK. Moreover, the structural analysis of synthesized nanoparticles was performed using transmission electron microscopy (by JEM-F200 apparatus, Japan). Also, the FTIR of the functional groups of the nanoparticle was determined through a Bruker Vector 22 wavelength (500-4000). Pore properties and specific surface area were determined by applying the BET test (Microtrac Bel Corp- model Belsorp mini II, Japan, Quanta Chrome).

### Preparation of Standard Solution

To prepare the standard solution of ibuprofen, the stages are as follows: dissolve 1.6 g of ibuprofen in 10 ml of 69% concentrated nitric acid, then add the solution to a 1000 ml volumetric flask. Afterward, the standard mother solution of 1000 mg l<sup>-1</sup> of ibuprofen is prepared [20]. Different masses of sorbent materials within the concentration range of 5-100 g l<sup>-1</sup> were put into contact with a 0.03 M KNO<sub>3</sub> solution. The aqueous suspensions were agitated for 24 h in a shaker at 250 rpm until equilibrium was reached. The pH<sub>pzc</sub> is the pH at which a plateau is achieved when plotting equilibrium pH versus sorbent mass.

### Adsorption Process

The intensity reduction curves and equilibrium sorption capacities were measured in batch tests through shaking, at certain times (5-240 min), experiment tubes comprising specific nanoadsorbent (wt.%), and 60 ml of drug solution. A magnet stirrer device was preferred to a conventional stirring apparatus in order to minimize the nanoparticle's sediment generation. The stirring rate was kept fixed at 500 rpm. These experiments were performed in an ambient room at 25 °C. Afterwards, aqueous specimens were taken, and filtered, and they were analyzed by spectrophotometry (Shimadzu, LAAN-A-AA-E001, Japan) at a wavelength of 222 nm to

determine the amount of drug contaminant removal. The kinetic data of the adsorbed quantity of ibuprofen at time  $t$ ,  $q_t$  ( $\text{mmol g}^{-1}$ ), was acquired by the mass equilibrium [21]:

$$q_t = \left( \frac{(C_0 - C_t)V}{m} \right) \quad (1)$$

where  $q_t$  is the adsorbed drug ( $\text{mmol/g}$  adsorbent) on the nanoadsorbent,  $m$  is the mass of nanoadsorbent ( $\text{g}$ ),  $V$  is the volume of drug contaminations ( $\text{l}$ ),  $C_0$  is the initial aqueous solution concentration ( $\text{mM}$ ), and  $C_t$  is the aqueous solution concentration ( $\text{mM}$ ) at any time. When  $t$  is equal to the equilibrium reaction time, then the value of the drug adsorbed at equilibrium,  $q_e$ , is determined by applying Eq. (1).

## Experimental Design

Response surface methodology (RSM) by central composite design (CCD) was applied for optimization of removal of ibuprofen in adsorption reaction through applying design expert software tool. Operating variables *i.e.* pH (A), contact time (B), nanoadsorbent dosage (C), and nanoadsorbent type (D) were changed to maximize the removal of drug contamination (Y). Table 1 revealed the coded and un-coded levels of central composite independent

parameters employed for the optimization of process variables in the removal of ibuprofen. The experimental design consisting of 38 test runs is presented in Table 2.

These tests were promoted to investigate the impact of each independent parameter (pH, contact time, nanoadsorbent dosage, and type of nanoadsorbent) and relations between these parameters on the removal of ibuprofen *i.e.* dependent parameter. Polynomial Eq. (2) was employed to investigate the empirical data by applying RSM regression [36]. In this equation,  $Y$  is the response parameter,  $b_0$  is intercepted,  $b_i$  is the first-order factor,  $X_i$  is an independent factor,  $b_{ii}$  is the second-order factor,  $b_{ij}$  is the linear term of the model for interaction between parameters,  $k$  is the number of variables examined also optimized [22].

$$Y = b_0 + \sum_{i=1}^k b_i X_i + \sum_{i=1}^k b_{ii} X_i^2 + \sum_{i=1}^k \sum_{j=i+1}^k b_{ij} X_i X_j \quad (2)$$

## RESULTS AND DISCUSSION

### Characterization of Nanoparticles

**X-ray diffraction.** An X-ray diffraction study was performed to demonstrate the crystalline nature of the ZnO nanoparticles after the formation of the nanoadsorbents.

**Table 1.** CCD Independent Parameters for Optimization of Reaction Parameters Adsorption Process

No.	Factor	Symbol	Scope				
			-2	-1	0	+1	+2
1	pH	A	3.32	4	5	6	6.68
2	Contact time (min)	B	6.59	10	15	20	23.41
3	Adsorbent dosage (wt.%)	C	0.01	0.02	0.03	0.04	0.05
4	Adsorbent type	D	ZnO/Fe <sub>2</sub> O <sub>3</sub>			ZnO/activated carbon	

**Table 2.** Surface Characteristics of ZnO/Fe<sub>2</sub>O<sub>3</sub> and ZnO/activated Carbon Nanoparticles Specified *via* BET Approach

Feature	ZnO/Fe <sub>2</sub> O <sub>3</sub>	ZnO/activated carbon
$V_m$ ( $\text{cm}^3$ (STP) $\text{g}^{-1}$ )	53.175	67.384
$a_{s, \text{BET}}$ ( $\text{m}^2 \text{g}^{-1}$ )	68.29	106.95
$a_{s, \text{Lang}}$ ( $\text{m}^2 \text{g}^{-1}$ )	154.57	208.43
Total pore volume ( $\text{cm}^3 \text{g}^{-1}$ )	0.1698	0.1725
Mean pore diameter (nm)	3.452	3.648

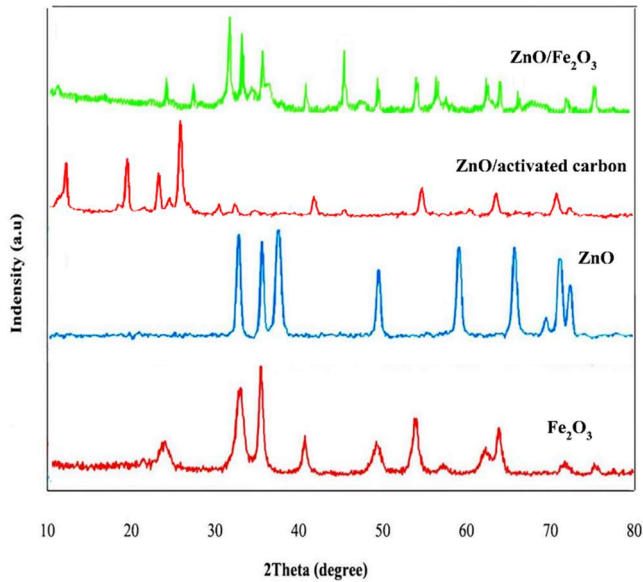


**Fig. 2.** XRD pattern for nano adsorbents.

Nevertheless, it was deemed necessary to first show the XRD patterns of the ZnO nanoparticles. As can be seen in Fig. 2, both pure ZnO and ZnO/Fe<sub>2</sub>O<sub>3</sub> have almost identical patterns, which are distinguished by the presence of the main peaks at about 2θ (25, 19, 33.76, 44.51, 56.38, and 67.43) for ZnO/Fe<sub>2</sub>O<sub>3</sub> [23]. On the other hand, both pure ZnO and ZnO/activated carbon show almost similar patterns characterized by the presence of the main different peaks at about 2θ equal to 12, 74, 20.93, 26.48, and 45.36 for ZnO/activated carbon. Moreover, the results of XRD analysis show that there is no structural change after the nano adsorbents and incorporation of Fe<sub>2</sub>O<sub>3</sub> and activated carbon. As displayed in Fig. 2, the nano adsorbents formation by ZnO nanoparticles on the external surface impact either on the ZnO/Fe<sub>2</sub>O<sub>3</sub> and ZnO/activated carbon nanoparticles phases or on the crystalline lattice of the nano adsorbents.

**SEM analysis.** The morphology of the synthesized nano adsorbents was determined by SEM analysis, as displayed in Fig. 3. According to this figure, it can be observed that the surface of the adsorbents before the adsorption reaction is heterogeneous and has an irregular surface and has many cavities, which can be a suitable space to absorb drug contaminants such as ibuprofen. These pores become almost dense at various adsorbents, especially at the nano adsorbent surface, which can lead to bonding and

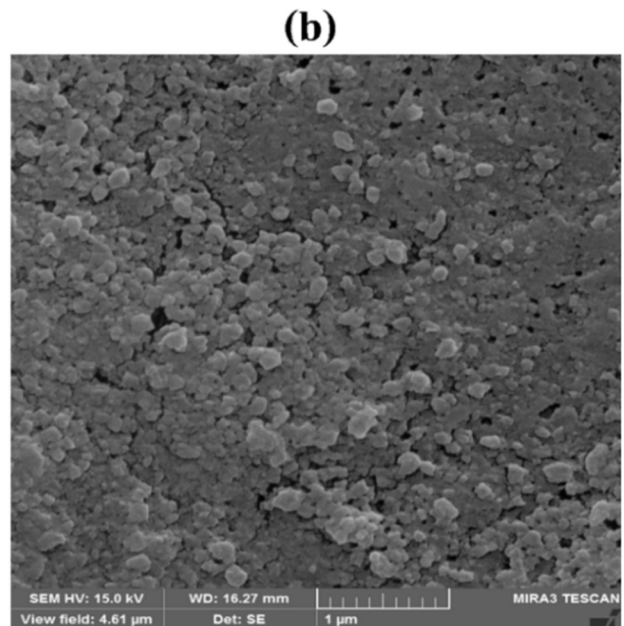
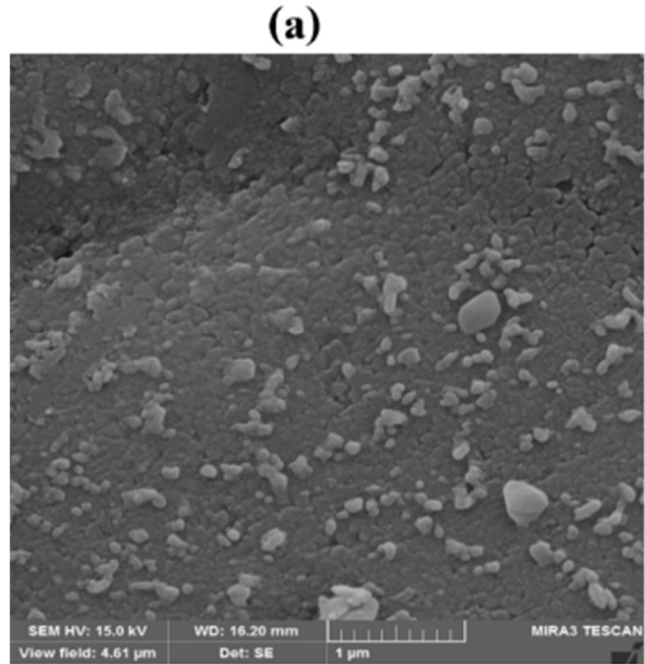


**Fig. 3.** SEM images of (a) ZnO/Fe<sub>2</sub>O<sub>3</sub>, (b) ZnO/activated carbon.

adsorption of drug contaminants on the adsorbent surface. Therefore, the adsorption phenomenon occurs by forming a complex between the surface of the nanoparticle and the ion [24].

**TEM analysis.** The structure of the prepared nanoadsorbents, which was analyzed utilizing TEM pictures, is displayed in Fig. 4. This figure represents both the nanoadsorbent with hexagonal structures. Through the incorporation of Fe<sub>2</sub>O<sub>3</sub> and activated carbon into the nanoadsorbent, a modification in structure can be achieved as recorded in Fig. 4b. In this figure, the nanoadsorbent morphology of the hexagonal-shaped construction can be observed. As shown in Fig. 4, ZnO/Fe<sub>2</sub>O<sub>3</sub> and ZnO/activated carbon nanoadsorbents have mean particle sizes of 80 and 70 nm, respectively.

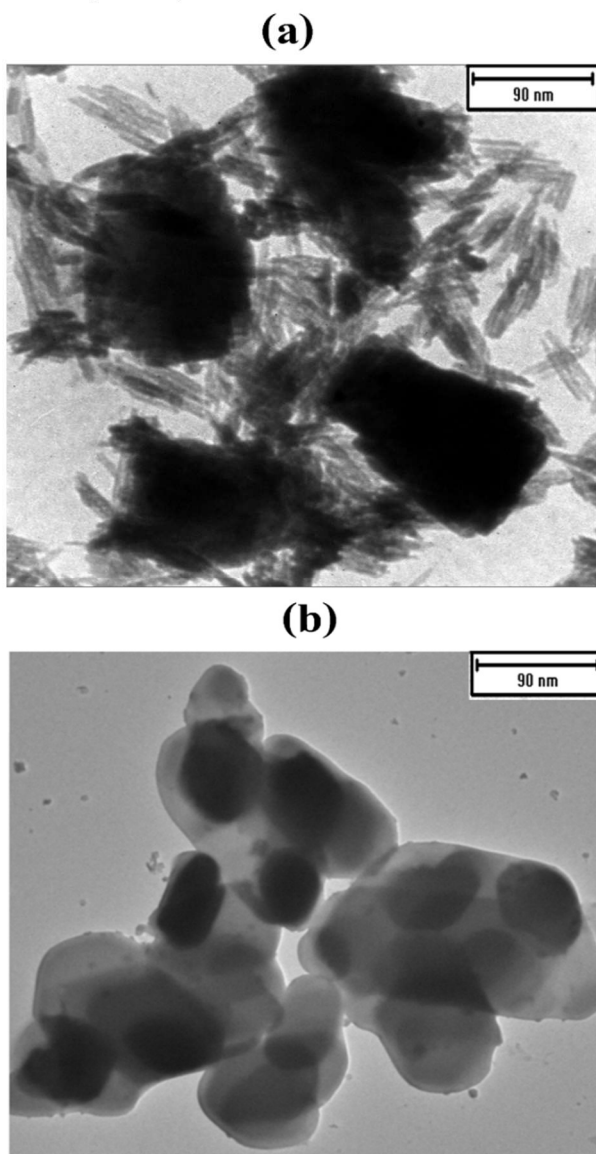


**Fig. 4.** TEM images of (a) ZnO/Fe<sub>2</sub>O<sub>3</sub>, (b) ZnO/activated carbon.

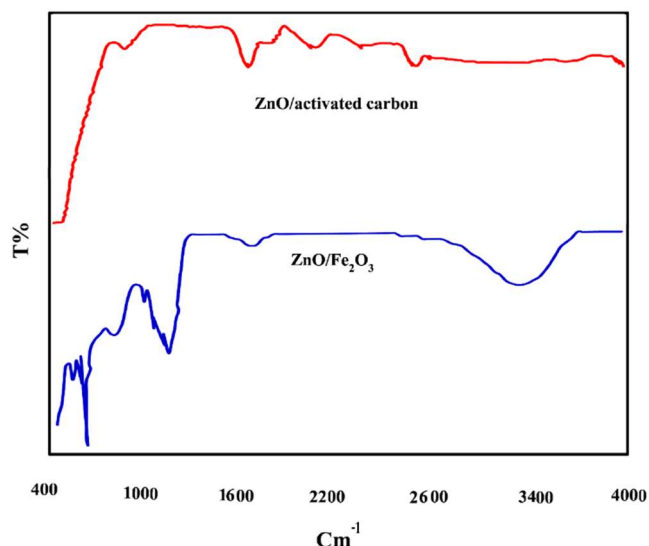


**Fig. 5.** FTIR graphs for the ZnO/Fe<sub>2</sub>O<sub>3</sub> and ZnO/activated carbon nanoadsorbents.

**FTIR analysis.** To specify the functional group present in the prepared nanoparticles, the FTIR spectrum of ZnO/Fe<sub>2</sub>O<sub>3</sub> and ZnO/activated carbon nanoadsorbents is illustrated in Fig. 5. The 984 cm<sup>-1</sup> band is related to C-O single bond [25]. The bands in the range of 2500-3500 cm<sup>-1</sup> are related to the OH stretching band in both photocatalysts. The band at 470 cm<sup>-1</sup> is owing to the vibration of the Zn-O functional group [26]. The band of 1002 to 1146 cm<sup>-1</sup> is attributed to the C-C bond of unsaturated groups on the surface of activated carbon. FT-IR outcomes indicated that acidic functional groups on the surface of nanoparticles were grown by acid activation, which can lead to a change in adsorbent activity [27].

**BET analysis.** The surface characteristics of ZnO/Fe<sub>2</sub>O<sub>3</sub> and ZnO/activated carbon nanoparticles such as S<sub>BET</sub>, the diameter of pores, and pore volume were specified by BET examination. According to Table 2, the specific surface area of ZnO/Fe<sub>2</sub>O<sub>3</sub> and ZnO/activated carbon nanoparticles were 68.29 and 106.95 m<sup>2</sup> g<sup>-1</sup>, respectively. Furthermore, the Langmuir-specific surface area of these nanoparticles was 154.57 and 208.43 m<sup>2</sup> g<sup>-1</sup>, respectively, demonstrating that ZnO/activated carbon has a higher specific surface area than ZnO/Fe<sub>2</sub>O<sub>3</sub>. In addition, the average pore diameter of ZnO/Fe<sub>2</sub>O<sub>3</sub> and ZnO/activated carbon nanoparticles were 3.452 and 3.648 nm, which proves that both nanoadsorbents

**Table 2.** Surface Characteristics of ZnO/Fe<sub>2</sub>O<sub>3</sub> and ZnO/activated Carbon Nanoparticles Specified via BET Approach

Feature	ZnO/Fe <sub>2</sub> O <sub>3</sub>	ZnO/activated carbon
V <sub>m</sub> (cm <sup>3</sup> (STP) g <sup>-1</sup> )	53.175	67.384
a <sub>s, BET</sub> (m <sup>2</sup> g <sup>-1</sup> )	68.29	106.95
a <sub>s, Lang</sub> (m <sup>2</sup> g <sup>-1</sup> )	154.57	208.43
Total pore volume (cm <sup>3</sup> g <sup>-1</sup> )	0.1698	0.1725
Mean pore diameter (nm)	3.452	3.648

have mesoporous structures. Also, the total pore volume of ZnO/Fe<sub>2</sub>O<sub>3</sub> and ZnO/activated carbon were 0.1698 and 0.1725 cm<sup>3</sup> g<sup>-1</sup>, respectively, indicating the high pore volume of these nanoparticles [28]. The proper S<sub>BET</sub> value and wonderful pore volume confirm that the ZnO/activated carbon is effective in the removal of ibuprofen through the adsorption technique.

### Model Validation

The phrases with a positive symbol reveal the synergistic impact that raises ibuprofen removal, while a negative symbol demonstrates an opposing impact. Table 4 displays the outcome of a statistical analysis of variance (ANOVA). It represented the importance of the fitness of the second-order model, the influence of unique phrases, and their interaction on the ibuprofen removal. The p-value estimated the importance of each regression coefficient. The second-order model with an F value of 46 and p-value <0.0001 for the empirical data implies that it is meaningful at a 94% certainty level. The pH (X<sub>1</sub>), contact time (X<sub>2</sub>), nanoparticle dosage (X<sub>3</sub>), and nano adsorbent type (X<sub>4</sub>) have a considerable effect on ibuprofen removal because of their low P-values [29]. Adjusted-R<sup>2</sup> with 0.9378 shows 93.78% mutability with the anticipated versus experimental values for ibuprofen removal described by the model. R<sup>2</sup> with 0.9596 exhibits a close accord between the anticipated and empirical values. Response Ibuprofen removal, Y explored by response surface design utilizing quadratic equation is illustrated using Eq. (3):

$$\text{Ibuprofen removal (\%)} = +78.75 + 9.45 A + 8.0 B + 3.84 C + 0.35 D - 4.93 AB + 2.90 AC - 2.29 AD + 0.98 BC - 1.56 BD + 1.15 CD - 10.70 A^2 - 8.38 B^2 - 8.21 C^2$$

(3)

Figure 6a demonstrates a normal probability plot of the residuals. The errors disperse normally beyond a straight line

and are unimportant. Besides, Fig. 6b illustrates the actual ibuprofen removal vs. anticipated ibuprofen removal. In order to be in accord with the experimental value, the anticipated ibuprofen removal must lie near the Y=X line. The model calculated response close to the actual data for the approach in the range investigated [29].

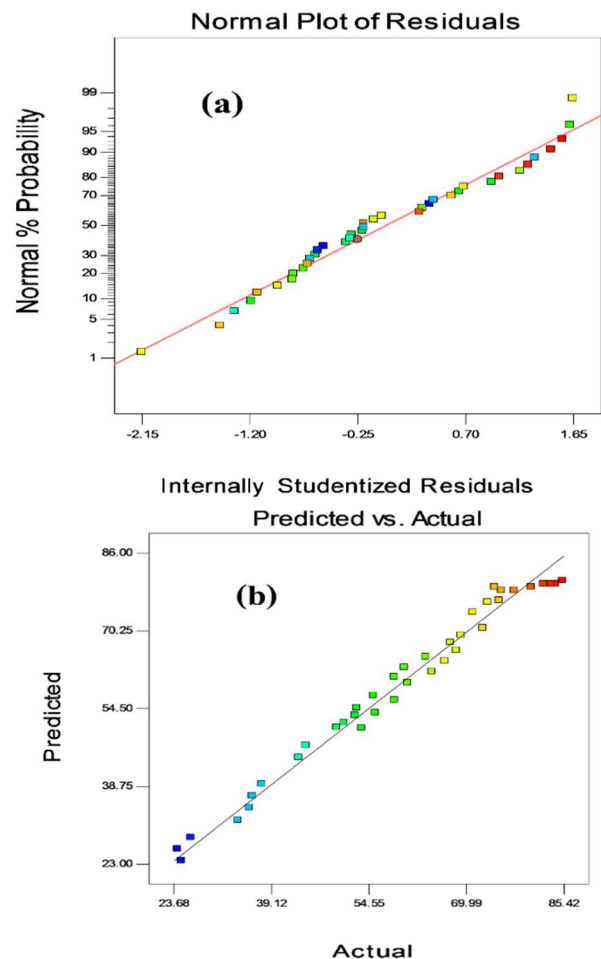


**Fig. 6.** (a) Normal probability plot of residual, (b) Predicted vs. actual ibuprofen removal.

**Table 3.** Experimental Design Matrix with CCD Method

run	pH	Contact time (min)	Dosage (g)	Adsorbent type	Ibuprofen removal (%)
1	4.00	20.00	0.02	Z/F	58.07
2	6.00	20.00	0.04	Z/C	71.05
3	4.00	10.00	0.04	Z/F	35.72
4	5.00	15.00	0.03	Z/C	84.31
5	5.00	15.00	0.03	Z/F	74.52
6	4.00	10.00	0.02	Z/F	36.31
7	5.00	6.59	0.03	Z/C	36.43
8	6.00	20.00	0.02	Z/F	50.67
9	4.00	20.00	0.04	Z/F	55.34
10	5.00	15.00	0.03	Z/C	82.46
11	4.00	20.00	0.02	Z/C	52.43
12	6.00	20.00	0.04	Z/F	69.22
13	6.00	10.00	0.04	Z/F	61.75
14	3.32	15.00	0.03	Z/F	36.16
15	5.00	23.41	0.03	Z/F	68.47
16	5.00	15.00	0.03	Z/F	70.39
17	5.00	15.00	0.03	Z/F	73.19
18	5.00	15.00	0.03	Z/C	75.62
19	6.68	15.00	0.03	Z/F	64.73
20	6.00	20.00	0.02	Z/C	58.64
21	5.00	15.00	0.05	Z/F	69.64
22	6.00	10.00	0.02	Z/C	55.64
23	4.00	10.00	0.02	Z/C	24.32
24	5.00	15.00	0.03	Z/F	85.42
25	5.00	15.00	0.05	Z/C	60.75
26	5.00	15.00	0.01	Z/C	49.51
27	5.00	15.00	0.03	Z/C	77.62
28	3.32	15.00	0.03	Z/C	26.42
29	5.00	15.00	0.03	Z/C	83.49
30	5.00	6.59	0.03	Z/F	43.54
31	5.00	23.41	0.03	Z/C	72.67
32	6.68	15.00	0.03	Z/C	67.54
33	5.00	15.00	0.01	Z/F	43.15
34	6.00	10.00	0.04	Z/C	60.25
35	4.00	10.00	0.04	Z/C	24.91
36	4.00	20.00	0.04	Z/C	52.67
37	5.00	15.00	0.03	Z/F	80.32
38	6.00	10.00	0.02	Z/F	53.49

Z/F mean ZnO/Fe<sub>2</sub>O<sub>3</sub> and Z/C mean ZnO/activated carbon.

**Table 4.** Results of Analysis of Variance

Source	Sum of squares	df	Mean square	F Value	p-value Prob > F
Model	10746.08	13	826.62	43.90	<0.0001
A-pH	2439.74	1	2439.74	129.56	<0.0001
B-Time	1749.13	1	1749.13	92.88	<0.0001
C-dose	402.06	1	402.06	21.35	0.0001
D-Adsorbent	4.70	1	4.70	0.25	0.6218
AB	388.09	1	388.09	20.61	0.0001
AC	134.10	1	134.10	7.12	0.0134
AD	143.78	1	143.78	7.63	0.0108
BC	15.21	1	15.21	0.81	0.3777
BD	66.63	1	66.63	3.54	0.0722
CD	35.84	1	35.84	1.90	0.1804
A2	3128.45	1	3128.45	166.13	<0.0001
B2	1918.87	1	1918.87	101.90	<0.0001
C2	1841.18	1	1841.18	97.77	<0.0001
Residual	451.95	24	18.83		
Lack of fit	246.74	16	15.42	0.60	0.8162
Pure error	205.21	8	25.65		
Cor total	11198.03	37			

### The Effect of Process Parameters on the Ibuprofen Removal

**pH effect.** Functional groups are strongly dependent on pH. The effect of this parameter depends directly on the competitiveness of hydrogen ions with the ions of adsorbed material on the active sites of the adsorbent surface. The effect of pH on the removal of the antibiotic ibuprofen by the two adsorbents ZnO/Fe<sub>2</sub>O<sub>3</sub> and ZnO/activated carbon was investigated in the range of 4 to 6. As can be seen in Figs. 7 and 8, the removal of ibuprofen decreases rapidly with increasing pH, while when the pH is further increased to about 5.5, the removal of ibuprofen decreases slowly. The competition between the hydroxide ions in the solution and the nano-adsorption sites for the placement of ibuprofen ions leads to M-OH bonding on the particle surface. This phenomenon reduces the transfer of ions to the adsorbent and reduces the removal efficiency of the drug from the solution by creating a stable condition in an aqueous solution. Besides, the effect of pH on the uptake of drug contaminants by adsorbents can be attributed to the separation or non-

separation of different groups [30]. At pH above  $Pk_a$ , these groups are mainly in the dissociated state and can exchange  $H^+$  with ions in the solution. However, at low pH, due to the lack of separation of these functional groups, it is not possible to establish a bond with drug ions [31]. Therefore, the adsorption efficiency is significantly reduced. On the other hand, at low pH the adsorbent surface is positive, so ions approaching the adsorbent with a positive charge lead to repulsion, and the adsorption efficiency decreases. Furthermore, as pH increases, the uptake efficiency of ibuprofen antibiotic increases, which may be because of reduced competition between protons and ions for active sites or a decrease in positive charge [32]. Indeed, with a pH at the point zero charge (pHpzc) of 5.49 and when the mixture pH is under 5.49, the surface of the ZnO/Fe<sub>2</sub>O<sub>3</sub> and ZnO/activated carbon adsorbents blocks becomes positively charged and enhances the electrostatic attractions with ibuprofen antibiotic molecules because its isoelectric point is around 3, improving, accordingly, the adsorption procedure [33]. In addition, when the solution pH was higher than 5.49,

the ZnO/Fe<sub>2</sub>O<sub>3</sub> and ZnO/activated carbon adsorbents surface is negatively charged, attracting more positively charged functional groups of ibuprofen antibiotic, leading to strong electrostatic attractions and further high adsorption capacities.

**Contact time effect.** The effect of contact time on the ibuprofen adsorption process is shown in Figs. 7 and 9. As can be seen from these figures, the removal of ibuprofen gradually increases with increasing contact time. However, as the contact time increases, the percentage of ibuprofen removed from the water decreases. The adsorption process of the antibiotic ibuprofen on the nanoadsorbent surface occurs in two fast and slow steps. The first step, which is slower, is related to the internal penetration of the ions. In the second step, when the active binding groups are in the cell wall of the adsorbent particles, it occurs faster. The high initial adsorption rate is due to the surface binding of the active groups with the ions. Therefore, with time, the efficiency of removal of the antibiotic ibuprofen decreases due to the reduction of active sites [33]. Furthermore, the fast absorption of the drug by the nanoadsorbent may be due to the large pores and cavities available to the adsorbents, which provide rapid penetration for ibuprofen adsorption at the pore sites. Therefore, in the absorption of drug pollutants, the rate of adsorption decreases with increasing contact time.

**Adsorbent dosage.** The dose of adsorbent is an important parameter for the rate of drug adsorption by nanoadsorbents. Determining the optimal amount of adsorbent lowers treatment costs and reduces environmental pollution [34]. In the adsorption of ibuprofen by ZnO/Fe<sub>2</sub>O<sub>3</sub> and ZnO/activated carbon nanoadsorbents, the adsorption efficiency is improved by gradually increasing the amount of nanoadsorbent, as shown in Figs. 8 and 9. The increase of adsorbent dose in the reactor enhances the concentration gradient between the liquid and solid mass, which leads to improved mass transfer rate and removal of diclofenac in the aqueous solution. On the other hand, the percentage of removal of the antibiotic ibuprofen does not decrease more slowly with a further increase in the amount of nanoadsorbent. The reason for the increase in adsorption capacity with increasing doses of nanoadsorbent is the larger number of sites available to the adsorbent [35]. In other words, as the adsorbent concentration increases, the number of non-porous sites

increases. Another reason for reducing the adsorption capacity or reducing the percentage of ibuprofen antibiotic removed from the aqueous solution is to reduce the possibility of the adsorbent colliding with the adsorbent. This possibility is due to the accumulation and massification of the adsorbent, which ultimately reduces the surface area and increases the length of the energy distribution path [36].

**Adsorbent type.** The type of adsorbent used for the adsorption process can have a significant impact on performance. Two types of nanoadsorbents were used in this study. Figures 7 to 9a and 7 to 8b refer to ZnO/activated carbon and ZnO/Fe<sub>2</sub>O<sub>3</sub> nanoadsorbents, respectively. As can be seen from these figures, the removal rate of the antibiotic ibuprofen is almost the same in the presence of both nanoadsorbents. However, in the series of experiments, the performance of ZnO/Fe<sub>2</sub>O<sub>3</sub> nanoparticles is better. The reason is the more active site in the nanoadsorbent. The more active site provides significant pores for the reaction of ibuprofen ions on the surface. In addition, strong interactions between zinc oxides and iron oxides can significantly delay the deactivation of the active sites [37]. Therefore, it was observed that the performance of the ZnO/Fe<sub>2</sub>O<sub>3</sub> nanoadsorbent was more satisfactory than that of ZnO/active carbon.

## Optimization

Process optimization was performed using the response surface methodology and the central composite design, as shown in Fig. 10. The results showed that the optimal conditions for values of pH, contact time, nanoparticles dosage, and nano adsorbent type were obtained to be 5.48, 17.22 min, 0.03 wt.%, and ZnO/Fe<sub>2</sub>O<sub>3</sub>, respectively. In order to confirm the performance of the model proposed using the response surface methodology, the experiment was repeated 3 times under optimal conditions. The average of the outcomes acquired in the optimal state demonstrated that the removal percentage of ibuprofen was 84.61%, which was closely in line with the predicted value. It should be noted that adsorbent type 1 means ZnO/Fe<sub>2</sub>O<sub>3</sub>.

## Adsorption Kinetics

The adsorption kinetic of ibuprofen antibiotic onto ZnO/Fe<sub>2</sub>O<sub>3</sub> and ZnO/activated carbon nanoadsorbent was

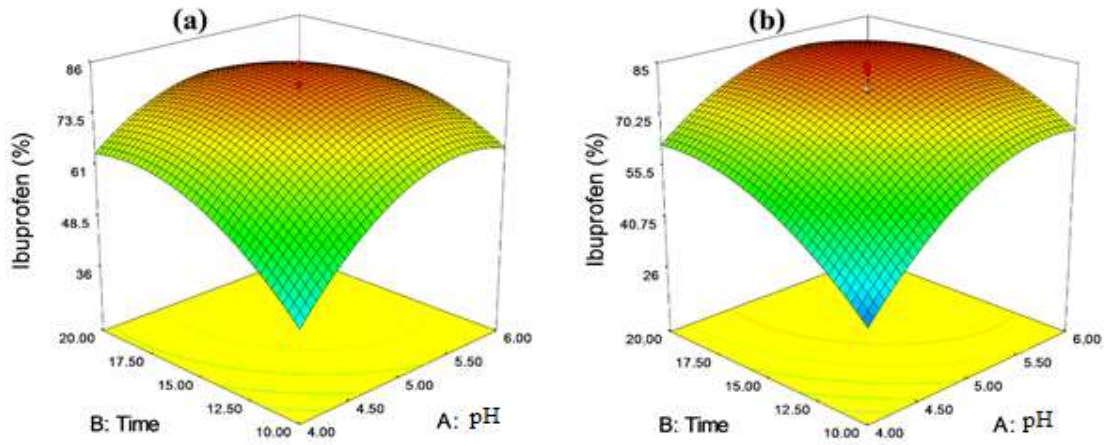


**Fig. 7.** Response surfaces and contour plots of ibuprofen removal: impact of pH and contact time on ibuprofen removal, (a) ZnO/activated carbon; (b) ZnO/Fe<sub>2</sub>O<sub>3</sub>. The dosage was fixed at zero level (0.03 g).

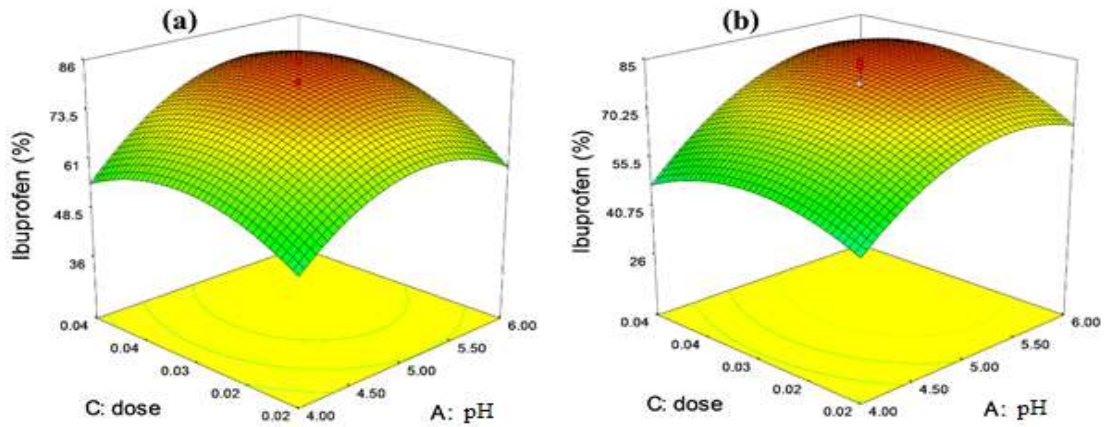


**Fig. 8.** Response surfaces and contour plots of ibuprofen removal: impact of pH and dosage on ibuprofen removal, (a) ZnO/activated carbon; (b) ZnO/Fe<sub>2</sub>O<sub>3</sub>. contact time was fixed at zero level (15 min).

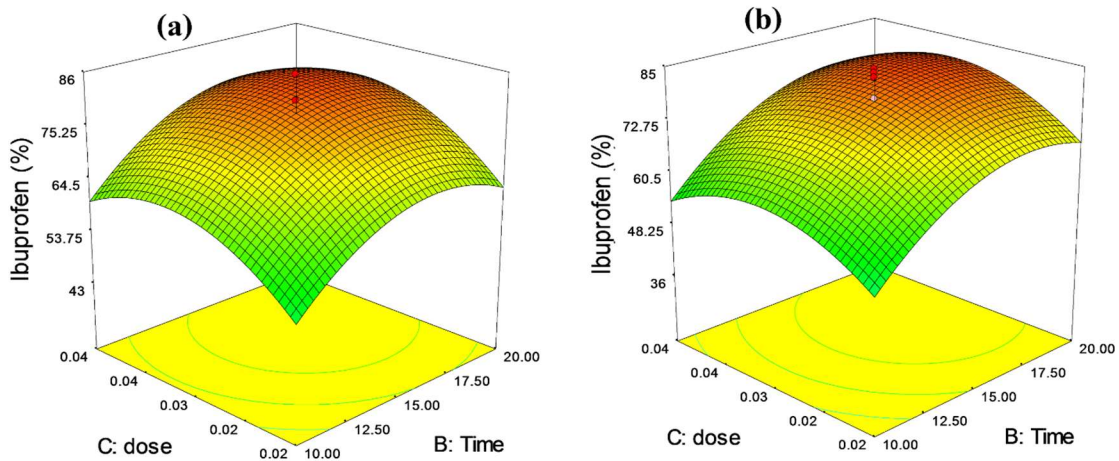


**Fig. 9.** Response surfaces and contour plots of ibuprofen removal: impact of contact time and dosage on ibuprofen removal, (a) ZnO/activated carbon; (b) ZnO/Fe<sub>2</sub>O<sub>3</sub>. pH was fixed at zero level (pH = 5).

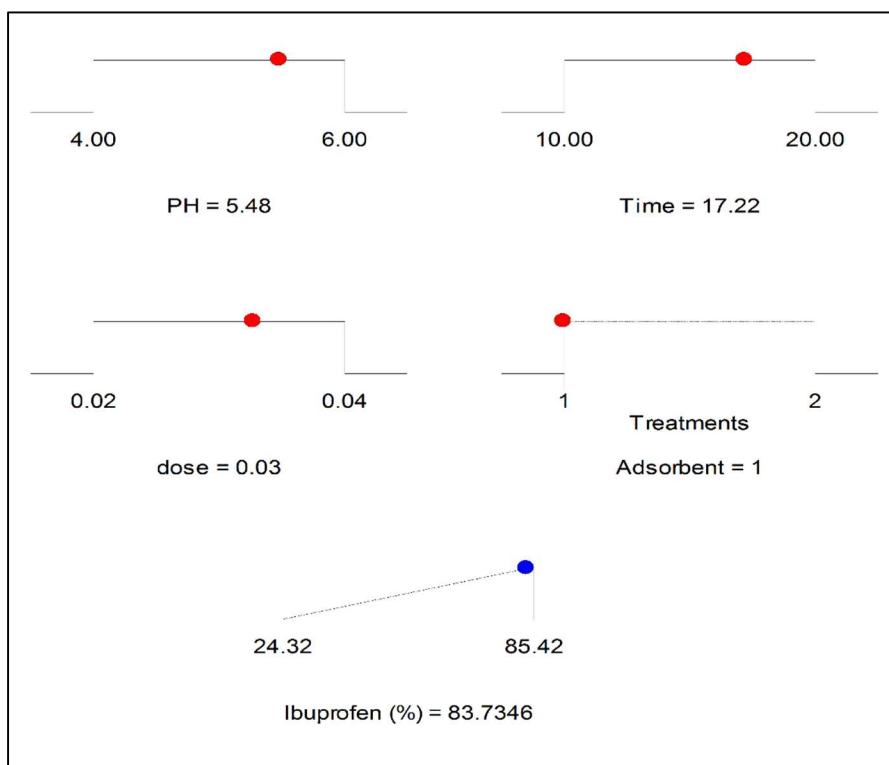


**Fig. 10.** Results of process optimization with response surface methodology and central composite design.

**Table 5.** Kinetic Parameters of Ibuprofen Adsorption onto ZnO/Fe<sub>2</sub>O<sub>3</sub> and ZnO/activated Carbon

	Pseudo-first order			Pseudo-second order		
	$q_{e1,cal}$ (mg g <sup>-1</sup> )	$K_1$ (min <sup>-1</sup> )	$R^2$	$q_{e1,cal}$ (mg g <sup>-1</sup> )	$K_2$ (g mg <sup>-1</sup> min <sup>-1</sup> )	$R^2$
ZnO/AC	8.61	0.0337	0.953	11.35	0.03	0.994
ZnO/Fe <sub>2</sub> O <sub>3</sub>	9.82	0.0356	0.926	9.18	0.024	0.996

examined employing both pseudo-first-order and pseudo-second-order kinetic models executed based on Eqs. (4) and (5), respectively [38].

$$\ln(q_e - q_t) = \ln q_e - k_1 t \quad (4)$$

$$\frac{t}{q_t} = \frac{1}{k_2 q_e^2} + \frac{t}{q_e} \quad (5)$$

where  $q_e$  and  $q_t$  are the values of ibuprofen drug adsorbed

onto nanoadsorbents at equilibrium and certain time  $t$ , respectively. Moreover,  $k_1$  (min<sup>-1</sup>) and  $k_2$  (g mg<sup>-1</sup> min<sup>-1</sup>) are the rate constant for the pseudo-first-order and pseudo-second-order adsorption, respectively. Table 5 demonstrates the tailored outcomes of both pseudo-first-order and pseudo-second-order kinetic models, while the assessed kinetic. According to the  $R^2$  comparison of the two models, it can be indicated that the amounts of the  $R^2$  achieved from the pseudo-second-order for both nanoadsorption are higher than those from the pseudo-first-order kinetics. The  $k_2$  amounts of

the pseudo-second-order kinetic equation (Table 5) were reduced with ibuprofen initial concentration increment, meaning that higher ibuprofen initial concentration needed more time to reach equilibrium [39]. Besides, the predicted and the experimental  $Q_e$  amounts are so close, which reveals that the ibuprofen adsorption kinetics on various nanoadsorption can be more precisely prognosticated by the pseudo-second-order model, proposing that the rate-controlling step might be chemisorption including chemical bonding between ibuprofen and the functional groups of nanoadsorption or exchange of electrons between them.

### Adsorption Isotherms

Langmuir and Freundlich isotherm forms represented *via* Eqs. (6) and (7), respectively, were applied to suitable the adsorption equilibrium isotherm of ibuprofen antibiotic onto both ZnO/Fe<sub>2</sub>O<sub>3</sub> and ZnO/activated carbon nano adsorbents at ambient temperature as illustrated in Table 6. It is well-founded that the Langmuir model assumes monolayer adsorption on adsorbents with uniform dispersal of sorption pores, while the Freundlich model can be employed to better express non-uniform cover adsorption [40].

$$\frac{C_e}{q_e} = \frac{1}{q_{max}K_L} + \frac{1}{q_{max}}C_e \quad (6)$$

$$\log(q_e) = \log(K_F) + \frac{1}{n}\log(C_e) \quad (7)$$

where  $q_e$  is the number of ibuprofen molecules adsorbed onto nano adsorbents at equilibrium.  $Q_{max}$  and  $K_L$  are the Langmuir constants for the adsorption capacity and adsorption velocity, respectively. While  $K_F$  is the adsorption capability of the adsorbent and  $n$  demonstrates the desirability of the adsorption reaction.

According to the  $R^2$  comparison of the two models, it can be found that the Langmuir model can superior match the

adsorption reaction of ibuprofen antibiotic, proposing its monolayer adsorption onto both ZnO/Fe<sub>2</sub>O<sub>3</sub> and ZnO/activated carbon nano adsorbents. Moreover, the outcomes demonstrated that the capacity maximum of Langmuir adsorption for ZnO/Fe<sub>2</sub>O<sub>3</sub> and ZnO/activated carbon nano adsorbents was achieved at 33.78 and 54.94 mg g<sup>-1</sup>, respectively.

### Comparison of Prepared Nano Adsorbents with other Adsorbents

The ibuprofen removal from ZnO/Fe<sub>2</sub>O<sub>3</sub> and ZnO/activated carbon nanoparticles was compared with other studies, as reported in Table 7. As reported, Asadi *et al.* acquired an ibuprofen removal of 99% employing LiY(MoO<sub>4</sub>)<sub>2</sub> QD/BioMOFs, which is higher than that of this investigation. Nevertheless, we obtained the ibuprofen removal of 83.74 and 85.42% after 17.22 min for ZnO/Fe<sub>2</sub>O<sub>3</sub> and ZnO/activated carbon nanoparticles, respectively. By comparing other adsorbents in ibuprofen removal, it is clear that ZnO/Fe<sub>2</sub>O<sub>3</sub> and ZnO/activated carbon nanoparticles have suitable efficiency in ibuprofen removal from water solution. Also, according to Table 7, compared to other nano adsorbents, ZnO/Fe<sub>2</sub>O<sub>3</sub> nanoparticles have a suitable adsorption capacity and ZnO/activated carbon nanoparticles have the highest absorption capacity among similar methods.

### CONCLUSIONS

The experimental study on the removal of the antibiotic ibuprofen was investigated using response surface methodology based on a central composite design. ZnO/Fe<sub>2</sub>O<sub>3</sub> and ZnO/activated carbon nanoadsorbents were synthesized as adsorbents. The nanoadsorbents were characterized by XRD, SEM, TEM, FTIR, and BET. The nanoparticle characterization results confirmed that the ZnO was successfully distributed in the structure of the

**Table 6.** Isotherm Parameters of Ibuprofen Adsorption onto ZnO/Fe<sub>2</sub>O<sub>3</sub> and ZnO/activated Carbon

	Langmuir model			Freundlich model		
	$q_m$ (mg g <sup>-1</sup> )	$K_L$ (l mg <sup>-1</sup> )	$R^2$	$K_F$ (l mg <sup>-1</sup> )	1/n	$R^2$
ZnO/AC	54.94	0.006	0.996	0.84	0.71	0.984
ZnO/Fe <sub>2</sub> O <sub>3</sub>	33.78	0.007	0.991	0.81	0.67	0.987

**Table 7.** Comparative Work with Reported Studies

Adsorbent type	Synthesis method	Antibiotic	Time (min)	Removal (%)	Adsorption capacity (mg/g)	Ref.
LiY(MoO <sub>4</sub> ) <sub>2</sub> QD/BioMOFs	Hydrothermal	Ibuprofen	60	99	14.17	[41]
Multi-walled carbon nanotubes	Chemical vapor deposition	Ibuprofen	40	74	37.59	[42]
Coconut shell-based activated biochar	Pyrolysis	Ibuprofen	90	81.61	12.16	[43]
Rape straw biomass fiber/ $\beta$ -CD/Fe <sub>3</sub> O <sub>4</sub>	-	Ibuprofen	50	83	48.29	[44]
Plane tree leaf-derived biochar	Pyrolysis	Ibuprofen	30	96.34	10.41	[45]
ZnO/Fe <sub>2</sub> O <sub>3</sub>	Sol-gel	Ibuprofen	17.22	83.74	33.78	This work
ZnO/activated carbon	co-precipitation	Ibuprofen	17.22	85.42	54.94	This work

nano-adsorbent. The quadratic model with  $R^2 = 0.9596$  indicates that the RSM can predict the empirical results with high precision. The conclusion indicates that the pH, contact time, nanoparticle dosage, and type of nano-adsorbent have a significant effect on the percentage removal of ibuprofen. A pH of 5.4, contact time of 17.22, duration of 3.3 min, nanoparticle dosage of 0.03 wt%, and ZnO/Fe<sub>2</sub>O<sub>3</sub> type nano-adsorbent were proposed to optimize the process parameters. The associated removal percentage of 83.74% was in good agreement with an empirical removal of 85.42% at optimal conditions. It can be concluded that ZnO/Fe<sub>2</sub>O<sub>3</sub> nanoparticles can be employed as an efficient and promising adsorbent to remove antibiotics.

## REFERENCES

- [1] J.A. Byrne, P.S.M. Dunlop, J.W.J. Hamilton, P. Fernandez-Ibanez, I. Polo-Lopez, P. K. Sharma, A.S.M. Vennard, *Molecules* 20 (2015) 5574.
- [2] Z. Song, H. Gao, W. Zhang, D. Wang, *J. Water Process Eng.* 36 (2020) 101399.
- [3] L. EL-Kaddadi, M. Asbik, N. Zari, B. Zeghmati, *Appl. Therm. Eng.* 122 (2017) 673.
- [4] O. M'ghari, F.S.A. Hassani, M.E.M. Mekhroum, N. Zari, R. Bouhfid, A. el K. Qaiss, *J. Energy Storage*. 35 (2021).
- [5] B. Srikanth, R. Goutham, R. Badri Narayan, A. Ramprasath, K.P. Gopinath, A.R. Sankaranarayanan, *J. Environ. Manag.* 200 (2017) 60.
- [6] H. Chakhtouna, H. Benzeid, N. Zari, A. el kacem Qaiss, R. Bouhfid, *Sep. Purif. Technol.* 266 (2021) 118592.
- [7] S. Liu, R. Ma, X. Hu, L. Wang, X. Wang, M. Radosz, M. Fan, *Ind. Eng. Chem. Res.* 59 (2020) 7046.
- [8] S. Wang, H. Zhang, H. Huang, R. Xiao, R. Li, Z. Zhang, *Process Saf. Environ. Prot.* 139 (2020) 218.
- [9] P. Yang, L. Rao, W. Zhu, L. Wang, R. Ma, F. Chen, G. Lin, X. Hu, *Ind. Eng. Chem. Res.* 59 (2020) 6194.
- [10] J. Dutta, A.A. Mala, *Water Sci. Technol.* 82 (2020) 401.
- [11] B. Maleki, S.S. Ashraf Talesh, *Fuel*. 298 (2021) 120827.
- [12] S. Wan, Z. Hua, L. Sun, X. Bai, L. Liang, *Process Saf. Environ. Prot.* 104 (2016) 422.
- [13] L. Limousy, I. Ghouma, A. Ouederni, M. Jeguirim, *Environ. Sci. Pollut. Res.* 24 (2016) 9993.
- [14] R. Li, Z. Wang, X. Zhao, X. Li, X. Xie, *Environ. Sci. Pollut. Res.* 25 (2018).
- [15] V.H. Ojha, K.M. Kant, *Phys. B Condens. Matter*. 567 (2019) 87.
- [16] H.P. Boehm, *Carbon* N. Y. 32 (1994) 759.
- [17] M. Zbair, A. El Hadrami, A. Bellarbi, M. Monkade, A. Zradba, R. Brahmi, *J. Environ. Chem. Eng.* 8 (2020) 103667.
- [18] A. Tomczyk, Z. Sokolowska, P. Boguta, *Rev. Environ. Sci. Biotechnol.* 19 (2020) 191.
- [19] F.R. Oliveira, A.K. Patel, D.P. Jaisi, S. Adhikari, H. Lu, K. Khanal, *Bioresour. Technol.* (2017).
- [20] Y. Xu, Y. Ma, H. Ji, S. Huang, M. Xie, Y. Zhao, H. Xu,

- H. Li, *J. Colloid Interface Sci.* 537 (2019) 101.
- [21] Y. Gao, Y. Li, L. Zhang, H. Huang, J. Hu, S.M. Shah, X. Su, *J. Colloid Interface Sci.* 368 (2012) 540.
- [22] S. Chandak, P.K. Ghosh, P.R. Gogate, *Process Saf. Environ. Prot.* 137 (2020) 149.
- [23] I.M. Al-Riyami, M. Ahmed, A. Al-Busaidi, B.S. Choudri, *Appl. Water Sci.* 8 (2018) 1.
- [24] S. Anand, A.P. Amaliya, M.A. Janifer, S. Pauline, *Mod. Electron. Mater.* 3 (2017) 168.
- [25] S. Alhan, M. Nehra, N. Dilbaghi, N. Kumar Singhal, Ki.H. Kim, S. Kumar, *Environmental Research.* 173 (2019) 411.
- [26] E. Altıntug, M. Yenigun, A. Sari, H. Altundag, M. Tuzen, T.A. Saleh, *Environ. Technol. Innov.* 21 (2021) 101305.
- [27] F. Marahel, M. Ghaedi, A. Ansari, *Synthesis and Reactivity in Inorg. Nano-Met. Chem.* 45 (2015).
- [28] Y. Zhang, P. Su, D. Weathersby, Q. Zhang, *Appl. Surf. Sci.* 501 (2020) 144217.
- [29] B. Maleki, S.S. Ashraf Talesh, *RE.* 182 (2022) 43.
- [30] Y. Liu, Y. Zhang, J.D. Feng, C.F. Li, J. Shi, R. Xiong, *J. Exp. Nanosci.* 4 (2009) 159.
- [31] L. Qian, W. Zhang, J. Yan, L. Han, W. Gao, R. Liu, M. Chen, *Bioresour. Technol.* 206 (2016) 217.
- [32] B. Maleki, S.S. Ashraf Talesh, *J. Chem. Pet. Eng.* 56 (2022) 189.
- [33] M. Li, D. Wei, T. Liu, Y. Liu, L. Yan, Q. Wei, B. Du, W. Xu, *Sep. Purif. Technol.* 227 (2019) 115696.
- [34] H. Li, S.A.A. Mahyoub, W. Liao, S. Xia, H. Zhao, M. Guo, P. Ma, *Bioresour. Technol.* 223 (2017) 20.
- [35] M. Zubair, N.D. Mu'azu, N. Jarrah, N.I. Blaisi, H.A. Aziz, M. A. Al-Harhi, *Water. Air. Soil Pollut.* 231 (2020).
- [36] S. Wacharasindhu, S. Likitmaskul, L. Punnakanta, K. Chaichanwatanakul, K. Angsusingha, C. Tuchinda, *J. Med. Assoc. Thail.* 57 (1985) 603.
- [37] B.M. Jun, Y. Kim, J. Han, Y. Yoon, J. Kim, C.M. Park, *Water (Switzerland).* 11 (2019) 1.
- [38] Z Anfar, M. Zbair, H. Ait Ahsiane, A. Jada, N. El Alem, *RSC Adv.* 10 (2020) 11371.
- [39] A. Boukhelkhal, O. Benkortbi, M. Hamadache, *Environ. Technol. (United Kingdom)* 40 (2019) 3328.
- [40] M. Zbair, Z. Anfar, H. Ait Ahsaine, N. El Alem, M. Ezahri, *J. Environ. Manage.* 206 (2018) 383.
- [41] F. Asadi, H. Forootanfar, M. Ranjbar, A. Asadipour, *Arab. J. Chem.* 13 (2020) 7820.
- [42] D. Balarak, F.K. Mostafapour, A. Joghataei, *Biosci. Biotechnol. Res. Commun.* 10 (2) (2017) 311.
- [43] P. Chakraborty, S. Show, W. Rahman, G. Halder, *PSEP.* 126 (2019) 193.
- [44] G. Wu, Q. Liu, J. Wang, S. Xia, H. Wu, J. Zong, J. Han, W. Xing, *Industrial Crops and Products.* 173 (2021) 114150.
- [45] X. Yang, X. Zhang, H.H. Ngo, W. Guo, J. Huo, Q. Du, Y. Zhang, C. Li, F. Yang, *J. Water Proc. Engineering.* 46 (2022) 102627.